



UvA-DARE (Digital Academic Repository)

Non-contact spectroscopic age determination of bloodstains

Bremmer, R.H.

Publication date
2011

[Link to publication](#)

Citation for published version (APA):

Bremmer, R. H. (2011). *Non-contact spectroscopic age determination of bloodstains*. [Thesis, fully internal, Universiteit van Amsterdam].

General rights

It is not permitted to download or to forward/distribute the text or part of it without the consent of the author(s) and/or copyright holder(s), other than for strictly personal, individual use, unless the work is under an open content license (like Creative Commons).

Disclaimer/Complaints regulations

If you believe that digital publication of certain material infringes any of your rights or (privacy) interests, please let the Library know, stating your reasons. In case of a legitimate complaint, the Library will make the material inaccessible and/or remove it from the website. Please Ask the Library: <https://uba.uva.nl/en/contact>, or a letter to: Library of the University of Amsterdam, Secretariat, P.O. Box 19185, 1000 GD Amsterdam, The Netherlands. You will be contacted as soon as possible.

The precise determination of chromophore concentration in scattering media is hampered by the influence of the setup geometry and the absorption on the path length distribution, $P(\ell)$, of the detected photons. We show that $P(\ell)$, as determined by Monte Carlo (MC) simulations for a non absorbing sample, can be used to describe the reflectance spectroscopy measurements as function of absorption by simply applying Beer's law. For low scattering ($\mu'_s=1 \text{ mm}^{-1}$) and high scattering ($\mu'_s=11.5 \text{ mm}^{-1}$), the simulated reflectance highly correlated with non-contact reflectance spectroscopy measurements without the use of fitting parameters. In hemoglobin containing samples we show that the simulated relation between reflectance and absorption can be used to determine the absorption spectrum of the medium without using additional light transport models. In conclusion, the reflectance spectroscopy signal as a function of absorption is completely determined by the photon path length distribution at zero absorption. The simulated reflectance ratios allow for rapid determination of absorption coefficients based on reflectance spectroscopy measurements of highly scattering samples.

CHAPTER 6
PHOTON PATH LENGTH DISTRIBUTION MODEL
FOR REFLECTANCE SPECTROSCOPY

Submitted to Optics Letters



INTRODUCTION

Conventional reflectance measurements are routinely used in medicine e.g. to determine the oxygen saturation of blood [69]. Applications of reflectance spectroscopy are not limited to determining oxygen saturation, but may also assist in determination of the age of bloodstains (Chapter 2) or bruises [99]. These measurements require translating reflectance spectroscopy values into absorption coefficients to determine the presence of clinically, or forensically relevant chromophores as (oxy)-hemoglobin, met-hemoglobin, bilirubin or hemichrome [97, 105, 125, 126] in highly scattering tissues. To enable differentiation between these chromophores, measurements over a large spectral range are required. The influence of the optical properties and probe geometry on the path length of the light travelling through the tissue under study results in a non-linear relation between reflectance and absorption. This relation can be determined by the diffusion approximation model, empirical model [105], or a lookup table [97]. An alternative approach, albeit time consuming, is performing MC simulations to determine the relationship between reflectance and absorption [125, 126]. In principle, reflectance spectra of absorbing tissues can be calculated by combining Beer's law of absorption with the path length distribution of the detected photons, $P(\ell)$, in non-absorbing tissues. $P(\ell)$ can be measured in a Mach-Zehnder setup [127] or by time resolved experiments [128]. The influence of absorption on these photon path length distributions can be measured [129] or simulated [130]. However these techniques are cumbersome and currently limited to a too small spectral wavelength range for chromophore identification. In this study, we show that by using $P(\ell)$ as determined by MC simulations, the effect of absorption on reflectance measurements can be precisely described. Vice versa, using $P(\ell)$, absorption spectra of scattering samples can be assessed over a sufficiently large spectral range for chromophore determination in tissues.

METHODS

Our setup geometry specific $P(\ell)$ was determined from a single MC simulation at zero absorption (so called white MC) with the proper fiber probe arrangement and optical properties (scattering, refractive index). The simulated ratios between the reflectance with and without the presence of absorption were compared with reflectance ratios measured on phantoms with low ($\mu'_s=1 \text{ mm}^{-1}$) and high ($\mu'_s=11.5 \text{ mm}^{-1}$) reduced scattering properties.

The reflectance spectra were recorded with a non-contact reflectance spectroscopy setup, containing a USB4000 spectrograph, DH-2000 light source and QR400-7-UV/BX probe, all from Ocean Optics. The probe, consisting of 6 illumination fibers surrounding the center detection fiber, was tilted 13° off-normal and positioned at a height of 17 mm above the phantom. This configuration makes the reflectance measurements insensitive to direct reflections and to changes in the probe position (Chapter 4). The reflectance spectra were recorded over the wavelength range of 400-900 nm, and averaged into bins of 10 pixels, which allowed calculation of a standard deviation.

Phantoms consisted of a mixture of Intralipid 20% (Fresenius, Kabi AG), phosphate buffered saline, and varying concentration of Evans Blue (Sigma Aldrich) to control the amount of absorption. Additional phantoms were prepared at the two selected μ_s' -values with no Evans Blue added, which were utilized to obtain baseline measurements, $R(\mu_s', \mu_a=0) = R_0$. Figure 1 shows typical reflectance spectra of two phantoms, without and with absorber added ($\mu_a = 0.2 \text{ mm}^{-1}$). First, we analyzed the data for a single wavelength, $\lambda=611 \text{ nm}$, for the Evans Blue phantoms at the maximum reflectance difference between the non-absorbing and absorbing phantoms. For instance, at $\lambda=611 \text{ nm}$, the reflectance of the phantom without absorber and $\mu_s'=1 \text{ mm}^{-1}$ is 0.071 and with absorber ($\mu_a = 0.2 \text{ mm}^{-1}$) 0.024, so the ratio R/R_0 is 0.34.

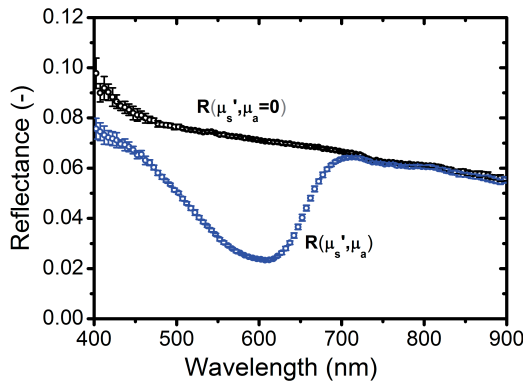


Figure 1. Reflectance spectra normalized to the reflectance of a SpectralonTM standard from an Intralipid solution ($\mu_s'=1 \text{ mm}^{-1}$ at 611 nm) without (black) and with Evans Blue added (blue, $\mu_a=0.2 \text{ mm}^{-1}$ at 611 nm).

Monte Carlo simulations with the experimental probe geometry, refractive index of 1.35 and a Henyey-Greenstein scattering phase function $g=0.75$ as input parameters were performed using the code of De Mul *et al* [132]. The reflectance signal in the absence of absorption R_0 , is the sum of the photon path length distribution over all path lengths:

$$R_0 = \sum_{\ell=0}^{\infty} P(\ell) \quad (1)$$

The simulation was terminated when 100,000 photons were collected ($R_0=100,000$). Knowledge of the path length distribution allows determination of the reflected signal in the presence of an absorber, by applying Beers law to all individual path lengths.

$$R = \sum_{\ell=0}^{\infty} P(\ell) \cdot \exp(-\mu_a \ell) \quad (2)$$

RESULTS

The reflectance ratio R/R_0 at a specific absorption is then calculated from Eq (2) and (1). Figure 2 shows the path length distributions $P(\ell)$ for the two scattering conditions $\mu'_s = 1$ and 11.5 mm^{-1} , and Figure 2 shows the path length distributions $P(\ell)$ for the two scattering conditions $\mu'_s = 1$ and 11.5 mm^{-1} , and for $\mu_a = 0$ and 1 mm^{-1} . The distribution of photon path lengths is very broad. For high scattering, $\mu'_s = 11.5 \text{ mm}^{-1}$, the most common path length is 0.54 mm , while the average photon length is 5 mm . Because of this wide range, the reflectance signal is sensitive to both very low and very high absorption. Please note that the number of photons detected remains finite for small photon path lengths, which can be attributed to our probe geometry in which the field of view of collection and delivery fiber overlap. Since diffusion theory requires a minimum of scattering events: $N \geq 4/(1-g)$ [133], and accordingly a minimal path length: $\ell \geq 4/\mu'_s$, this requirement excludes application of diffusion theory, neither as time resolved [134] nor as steady state [100].

The sum of all counts over all photon path lengths accumulates to the total number of photons detected. Figure 3 compares the measured reflectance ratios at $\lambda=611 \text{ nm}$ with the simulated ratio (Eq (2) over Eq. (1)) for absorption coefficients varying between $\mu_a = 0.1$ and 20 mm^{-1} for both the low and high scattering conditions. Please note the excellent agreement between experiment as shown in figure 1 and simulation. Good correspondence between measurements and simulations is found for large range of absorption coefficients without the use of fitting parameters (Pearson correlation coefficient, r^2 , of 0.997 for $\mu'_s = 1 \text{ mm}^{-1}$ and 0.998 for $\mu'_s = 11.5 \text{ mm}^{-1}$). Still, at large absorption values and low scattering the agreement between measurements and simulations deviates, which is merely attributed to the low signal to noise level of the reflected light, and can be minimized by measuring dark references, as described in [105].

Next we performed the reverse procedure, recovering absorption spectra from an analysis of the data over the full spectral range. To validate our method on a blood

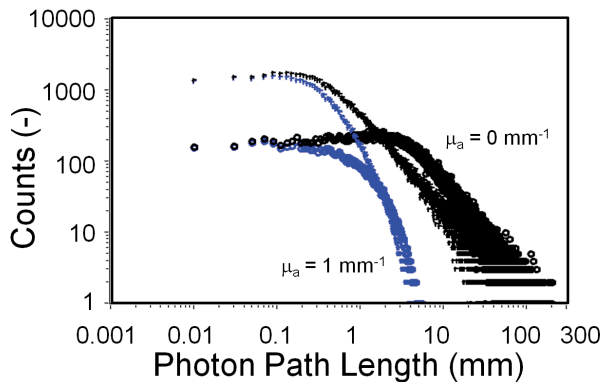


Figure 2. MC simulated photon path length distributions for non-contact reflectance spectroscopy for $\mu'_s = 11.5 \text{ mm}^{-1}$ (+) and for $\mu'_s = 1 \text{ mm}^{-1}$ (o) without (black) and with absorption (blue, $\mu_a = 1 \text{ mm}^{-1}$).

resembling phantom, we performed additional spectral measurements on a phantom containing Intralipid ($\mu_s' = 11.5 \text{ mm}^{-1}$ at 611 nm) and 27 mg/ml oxy-hemoglobin (HbO_2).

Figure 4 (top panel) shows the normalized reflectance spectra of Intralipid without and with HbO_2 added. Based on the measured reflectance ratio of figure 4A and the simulated relation between the reflectance ratio and absorption for $\mu_s' = 11.5 \text{ mm}^{-1}$ depicted in figure 3, the absorption spectrum of HbO_2 can be recovered for the entire wavelength range of 400-900 nm (figure 4B) panel). Again, good agreement is observed between assessed and literature HbO_2 absorption [31] for a large range of absorption coefficients ($r^2 = 0.974$). Yet, μ_s' decreases with increasing wavelength, which is not

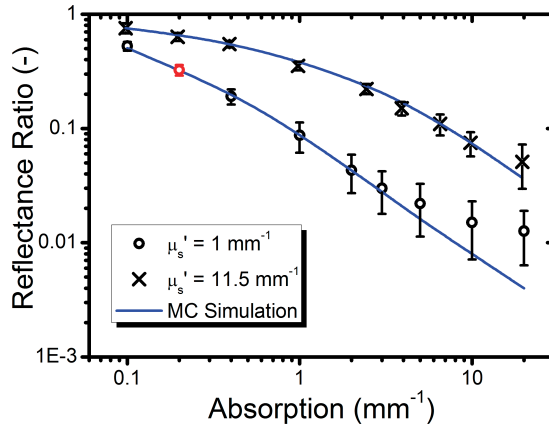


Figure 3. Reflectance ratio R/R_0 at various absorption values for high scattering (x, $\mu_s' = 11.5 \text{ mm}^{-1}$) and low scattering (o, $\mu_s' = 1 \text{ mm}^{-1}$) as measured at $\mu = 611 \text{ nm}$ and as determined by MC simulations (blue lines). Red dot resembles measurement from figure 1.

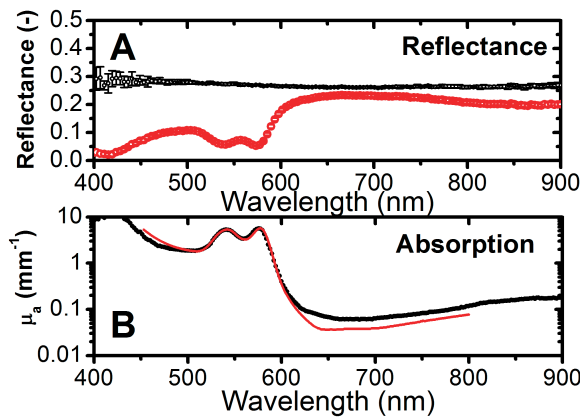


Figure 4. A) Normalized reflectance spectra from Intralipid solutions ($\mu_s' = 11.5 \text{ mm}^{-1}$ at 611 nm) without (black) and with HbO_2 added (red) B) Absorption of HbO_2 as assessed from reflectance measurements (black dots), and from literature (red line) [31].

accounted for in figure 4B. This induces the absorption to be underestimated at shorter wavelengths, and slightly overestimated at longer wavelengths.

DISCUSSION AND CONCLUSION

Comparison between white MC simulations and reflectance measurements requires measuring a reference reflectance at zero absorption. In virtually all clinical reflectance measurements another e.g. contra lateral location exists where the optical properties (refractive index and tissue scattering) can be considered virtually identical to those of the target tissue. Examples are forensic bloodstain studies on a cotton background [124], bruises from physical abuse on the body [99], and facial port wine stains [135]. Here, the reflectance spectrum of the other, virtually identical location may then serve as the R_0 . However, a small correction of the endogenous absorption, in skin the natural amount of blood (volume fraction of ~ 0.01) and melanin, over the spectral range may then be needed. From the ratio R/R_0 the absorption coefficient can be determined, which can then be used to identify the concentrations of chromophores present in the tissue under study. Measuring the local reference reflectance may eliminate the use of Spectralon™ reference, since this measurement value would be divided out when calculating the ratio.

We have shown the influence of absorption on the photon path length distribution. Next, the influence of scattering on $P(\ell)$ has to be determined. The relation between photon path length distribution and reduced scattering might be complicated and is topic of future study. Eventually, the μ_s' of the tissue under study also has to be estimated or measured. For high μ_s' the reflectance becomes insensitive for changes in μ_s' (Chapter 4), and estimation would be sufficient. Yet for low scattering coefficients, μ_s' and g could be measured by a different techniques, as low coherence spectroscopy [136] or optical coherence tomography [137] and subsequently simulated by a white MC. Another option might be to build a database of $P(\ell)$ for a range of μ_s' value or to measure $P(\ell)$ experimentally [129].

In conclusion, the reflectance spectroscopy signal as a function of absorption is completely determined by the photon path length distribution at zero absorption. The simulated reflectance ratios allow for rapid determination of absorption coefficients based on reflectance spectroscopy measurements of highly scattering samples.